







RESEARCH ARTICLE | JUNE 30 2023

# Identification of four detrimental chemicals using square-core photonic crystal fiber in the regime of THz

Abdulkarem H. M. Alkawani ; Dana N. Alhamss ; Sofyan A. Taya  ; Ayman Taher Hindi; Anurag Upadhyay; Shivam Singh; Ilhami Colak; Amrindra Pal ; Shobhit K. Patel 

 Check for updates

*Journal of Applied Physics* 133, 243103 (2023)

<https://doi.org/10.1063/5.0152927>



View Online



Export Citation

CrossMark

## AIP Advances

### Why Publish With Us?

 <b>25 DAYS</b> average time to 1st decision	 <b>740+ DOWNLOADS</b> average per article	 <b>INCLUSIVE</b> scope
--	--	---

[Learn More](#)

 AIP Publishing

# Identification of four detrimental chemicals using square-core photonic crystal fiber in the regime of THz

Cite as: J. Appl. Phys. **133**, 243103 (2023); doi: [10.1063/5.0152927](https://doi.org/10.1063/5.0152927)

Submitted: 3 April 2023 · Accepted: 10 June 2023 ·

Published Online: 30 June 2023



Abdulkarem H. M. Alkawgani,<sup>1</sup> Dana N. Alhamss,<sup>2</sup> Sofyan A. Taya,<sup>2,a)</sup> Ayman Taher Hindi,<sup>1</sup>  
Anurag Upadhyay,<sup>3</sup> Shivam Singh,<sup>4</sup> Ilhami Colak,<sup>5</sup> Amrindra Pal,<sup>6</sup> and Shobhit K. Patel<sup>7</sup>

## AFFILIATIONS

<sup>1</sup>Electrical Engineering Department, College of Engineering, Najran University, Najran, Kingdom of Saudi Arabia

<sup>2</sup>Physics Department, Islamic University of Gaza, P.O. Box 108, Gaza, Palestine

<sup>3</sup>Department of Applied Science and Humanities, Rajkiya Engineering College, Azamgarh, Uttar Pradesh, India

<sup>4</sup>Department of Electronics and Communication Engineering, ABES Engineering College, Ghaziabad, Uttar Pradesh, India

<sup>5</sup>Department of Electrical and Electronics Engineering, Nisantasi University, Istanbul, Turkey

<sup>6</sup>Department of EECE, School of Engineering and Technology, DIT University, Dehradun, Uttarakhand 248009, India

<sup>7</sup>Department of Computer Engineering, Marwadi University, Rajkot 360003, India

<sup>a)</sup>Author to whom correspondence should be addressed: [staya@iugaza.edu.ps](mailto:staya@iugaza.edu.ps)

## ABSTRACT

Numerous techniques and technologies have been proposed for the detection and identification of hazardous chemicals that can harm the lungs and respiratory system as well as the central nervous system and kidneys when inhaled. Most practical techniques can be carried out by extraordinary professionals in well-equipped facilities. A reliable, simple, highly sensitive, and feasible sensing technique is still required. A potential sensor for these harmful chemicals is the photonic crystal fiber (PCF), which achieves several unique properties. A square-core PCF sensor is proposed in this work for the detection of detrimental gases (tetra-chloro silane, tetra-chloro methane, turpentine, and tin terra-chloride) in the THz region. The cladding region is divided into three rings, and each ring has rectangular and square air holes. Within the operating region, we have found a relatively high sensitivity of 96.185% along with 95.407% core power fraction, 0.2211 numerical aperture, and a low effective area of  $154\,470\ \mu\text{m}^2$  at 1.9 THz frequency. Ignorable confinement loss of  $3.071 \times 10^{-14}\ \text{cm}^{-1}$  and effective material loss of  $0.007\,72\ \text{cm}^{-1}$  have been also found. Additionally, the current manufacturing techniques guarantee the viability of the proposed PCF sensor's manufacture. These obtained results demonstrate that the proposed sensor can be effectively employed for applications involving hazardous chemical compounds, gases, and biosensing.

Published under an exclusive license by AIP Publishing. <https://doi.org/10.1063/5.0152927>

## I. INTRODUCTION

Tetra-chloro methane ( $\text{CCl}_4$ ), tetra-chloro silane ( $\text{SiCl}_4$ ), tin terra-chloride ( $\text{SnCl}_4$ ), and turpentine ( $\text{C}_{10}\text{H}_{16}$ ) are chemical compounds that are widely used in the industrial sector.<sup>1,2</sup> The chemical compound tetra-chloro methane is also known as carbon tetrachloride. It is a colorless liquid with a sweet fragrance. At lower temperatures, it has no combustion potential. Due to safety and environmental concerns, it has now been phased out of use in cleaning agents, fire extinguishers, and as a precursor to refrigerants. High levels of carbon tetrachloride exposure, including its

vapor form, can damage the liver and kidneys as well as the central nervous system. Long-term exposure can be fatal. Tetra-chloro silane, often known as silicon tetrachloride, is an inorganic chemical having the formula  $\text{SiCl}_4$ . It is a volatile colorless liquid that fumes in the air. It is used for the production of silica and high-purity silicon for industrial applications. In China, pollution from silicon tetrachloride manufacture has been linked to the rise in the solar cell demand. According to the Material Safety Data Sheet, the inhalation of silicon tetrachloride results in burning sensation and sore throat. Tin terra-chloride is a colorless hygroscopic liquid

30 June 2023 09:58:53

inorganic compound. It fumes upon contacting the air. It is used as a precursor to other tin compounds. It was utilized in World War I as a chemical compound because when it comes into contact with air, it produces an irritating dense smoke. This smoke is not fatal. Turpentine is a substance made by distilling resin from living trees, primarily pines. It serves primarily as a specialized solvent but can also serve as a raw material for the chemical synthesis. As an organic solvent, its vapor can harm the lungs and respiratory system as well as the central nervous system and kidneys when inhaled.

Numerous techniques and technologies have been proposed for the detection and identification of hazardous substances. High detection sensitivity has been attained using liquid chromatography.<sup>3</sup> However, this practical technique can be carried out by extraordinary professionals in well-equipped facilities. With required tools, this process needs preparation, which makes it time-consuming. We require a reliable, highly sensitive, and feasible approach because of these factors. Up to now, the development of optical techniques is widely going in the field of analytical chemistry. A potential sensor for these harmful chemicals is photonic crystal fiber (PCF). PCF achieves several unique properties, including increased stability, design resilience, relative ease of use, robustness, etc. Due to these properties, PCF can be used in several applications.<sup>4–7</sup> These applications were not possible with usual optical fibers.<sup>8</sup> Researchers have become interested in the applications of PCFs more and more due to their unique properties. To improve sensing performance, researchers have recently proposed a range of PCF-based chemical sensor architectures.<sup>9–16</sup> The transition region of electronics and photonics can be established after linking the gap between microwave and infrared regions. This can be achieved with the terahertz (THz) frequency spectrum. This range of frequencies can offer some surprising potentials for the characterization of skin cancer detection, biological material detection, detection of explosives, and most significant chemical sensing.<sup>17,18</sup> Recently, a PCF-based sensor was proposed for the detection of sulfur dioxide as one of the major air pollution contributors. The numerical investigation was carried out in the spectral range from 0.8 to 1  $\mu\text{m}$ . A highest sensitivity of 59.34% was obtained in this work.<sup>19</sup> In another work, a side-polished birefringent PCF was proposed for sensing applications. The polished face of the PCF structure is coated with an indium tin oxide layer to stimulate surface plasmon. The analytes were placed on the flat face of the PCF.<sup>20</sup> More fields can be coupled to the ITO–dielectric interface due to the structure's birefringence. A sensitive PCF for the detection of humidity was proposed and numerically analyzed. The cladding of the PCF was coated with a graphene layer and a silver film. The outermost layer is coated with an agarose gel material to form a layer that is very sensitive to moisture.<sup>21</sup> The above-mentioned detrimental chemicals serve as silent executioners and pose a serious threat to people's health.<sup>22,23</sup> Therefore, a robust and perfect detection method for these harmful compounds is urgently needed. To cope with this issue, we propose a square-core PCF as a chemical detector.

In this paper, a square-core PCF is proposed and numerically analyzed for the detection of different chemicals, namely,  $\text{CCl}_4$ ,  $\text{SiCl}_4$ ,  $\text{SnCl}_4$ , and  $\text{C}_{10}\text{H}_{16}$ . The primary objective of constructing the proposed sensor is to detect detrimental chemicals that can be widely found in the industry sector. They can seriously harm

people when exposed to them. Cancer and damage to the liver, kidneys, eyes, and nervous system are few of the consequences of the exposure. The remaining sections of this article are arranged as follows. Section II describes the proposed sensor design parameters. The fabrication feasibility is also provided in this section. Section III highlights the calculation techniques for various PCF optical properties. The results from the current study are thoroughly discussed in Sec. IV, and we also compare these results with earlier published works. A brief conclusion is provided in Sec. V.

## II. DESIGN CONSIDERATION

### A. Model design

The design mechanism of the proposed sensor is described in this section. Typically, two steps are required to fully investigate the issue. The first step is using the finite element method to design the elementary structure, while the second one is to plot the various optical properties. The proposed PCF has a square core ( $s_1$ ) with 470  $\mu\text{m}$  side length and is designed with air cavities in both square and rectangular shapes in the cladding region. The cladding region has three rings. Four squares ( $s_2$ ) and four rectangles ( $r_1$ ) are organized in the first ring of the cladding area, with each square having a side length of 240  $\mu\text{m}$  and each rectangle having a height and width of 500 and 240  $\mu\text{m}$ , respectively. Four identical squares ( $s_2$ ) of a side length of 240  $\mu\text{m}$  and four identical rectangles ( $r_2$ ) are grouped in the second ring of the cladding area. The height and width of each rectangle ( $r_2$ ) are 1120 and 240  $\mu\text{m}$ , respectively. The third ring in the cladding region is composed of four rectangles ( $r_3$ ), each 220  $\mu\text{m}$  in width and 850  $\mu\text{m}$  in height. The fiber has a radius of 1250  $\mu\text{m}$ , and a 125  $\mu\text{m}$  thick PML is applied to prevent light scattering from the fiber. We have chosen a 10% radius of the entire fiber as the PML since an ideal selection of PML is necessary for effective loss measurement. All the parameters employed in the PCF-based sensor are displayed in Table I. Any type of sensing application raises questions about fiber material selection. Zeonex has been chosen as the fiber material for our investigation. This polymer material was chosen for several reasons. First, it exhibits a constant refractive index (REIX) of 1.53 in the THz regime. Second, it shows a minimal bulk absorption loss and a higher glass transition temperature. Figures 1(a) and 1(b) show the proposed structure, and its extremely fine mesh is shown in Fig. 1(c). The extremely fine mesh is applied, and it is found to have 13 078 domain elements and 1636 border elements.

### B. Fabrication feasibilities

One of the most significant issues in sensor usability is its fabrication feasibility. To ensure safe production without any damage, researchers are working to keep their designs as straightforward as they can. 3D printing, extrusion, stack and drilling, capillary stacking, and solgel are some of the widely utilized fabrication techniques used for PCF manufacturing. Solgel technique and capillary stacking make it simple to create circular-shaped PCFs. Some structures, such as PCFs with rectangular, elliptical, or square shapes, can be fabricated using extrusion and 3D printing technologies. The proposed structure has been selected to guide the light tightly inside the PCF core and to detect these harmful chemicals since

TABLE I. The parameters used in the proposed PCF.

Length of $s_1$	470 $\mu\text{m}$
Length of $s_2$	240 $\mu\text{m}$
Height of $r_1$	500 $\mu\text{m}$
Width of $r_1$	240 $\mu\text{m}$
Height of $r_2$	1120 $\mu\text{m}$
Width of $r_2$	240 $\mu\text{m}$
Height of $r_3$	850 $\mu\text{m}$
Width of $r_3$	220 $\mu\text{m}$
Distance between the core and air holes	35 $\mu\text{m}$
Distance between adjacent air holes	20 $\mu\text{m}$
R	1250 $\mu\text{m}$
PML	125 $\mu\text{m}$
$\alpha_{\text{Zeonex}}$	0.2 $\text{cm}^{-1}$
$n_{\text{Zeonex}}$	1.53
$n_{\text{SiCl}_4}$	1.411 56
$n_{\text{CCl}_4}$	1.461
$n_{\text{C}_{10}\text{H}_{16}}$	1.472
$n_{\text{SnCl}_4}$	1.5086

they have relatively high REIX. The Max Plank Institute recently produced a variety of complex-designed PCF structures. Since our proposed PCF sensor contains square and rectangular air holes, the aforementioned technologies, more notably the 3D printing and extrusion techniques, ensure the fabrication possibilities of this proposed sensor.

### III. METHODOLOGY

The chemical analyte is first introduced into the PCF core in order to begin the analysis. The speed of light in a medium is determined by its REIX. The performance of the sensor can be assessed based on specific sensing properties such as confinement loss, relative sensitivity, effective area, power ratio, and effective material loss. Relative sensitivity is the most significant characteristic. Typically, sensing is carried out by comparing the REIX. To calculate the relative sensitivity, one must calculate the light intensity that directly interacts with the sensor analyte. The power ratio (PF), which is used to measure the light extent associated with the analytes in the core, has a substantial impact on relative sensitivity. The power factor is given by<sup>16</sup>

$$PF = \frac{\int_{\text{analyte}} \text{Re}\{E_x H_y - H_x E_y\} dx dy}{\int_{\text{total}} \text{Re}\{E_x H_y - H_x E_y\} dx dy}, \quad \% \quad (1)$$

where the amount of light propagating in the core and total cross-sectional regions of the PCF are represented by the numerator and denominator, respectively.

The following equation is used to determine the relative sensitivity (RS) to an analyte where  $n_r$  and  $n_{\text{eff}}$  are the analyte and the effective modal REIX,<sup>17</sup>

$$RS = \frac{n_r}{n_{\text{eff}}} PF, \quad \% \quad (2)$$

Confinement loss (CL) is the loss that results from the optical confinement decreasing due to the cladding-core configuration of the PCF. The amount of light that is collected by air holes of the cladding area serves as a measure of this loss. When the CL is lower, the sensor quality will be higher. The CL is calculated by using<sup>18</sup>

$$CL = 8.686 \times k_0 \times \text{Im } \text{ginary}(n_{\text{eff}}) \times 10^{-2}, \text{ cm}^{-1}, \quad (3)$$

where  $k_0 = 2\pi/\lambda$ ,  $\lambda$  is the light wavelength and  $\text{Im } \text{ginary}(n_{\text{eff}})$  is the imaginary part of the modal REIX.

Sometimes, light can propagate out from the analyte in the core region. The zone where analyte sensing is most efficient is known as the effective area (EA) sometimes denoted as  $A_{\text{eff}}$ . A high-power density in the zone can be created by a lower EA with a significant nonlinear effect.  $A_{\text{eff}}$  can be expressed as<sup>16</sup>

$$A_{\text{eff}} = \frac{(\int |E^2| dx dy)^2}{\int |E^4| dx dy}, \quad \mu\text{m}^2. \quad (4)$$

A substantial amount of loss can be added to a PCF sensor due to the background substance. The loss that comes from the background substance is called effective material loss (EML). It can be dramatically reduced by reducing the amount of background substance. EML can be evaluated using<sup>17</sup>

$$EML = \frac{\sqrt{\frac{\epsilon_0}{\mu_0}} \int_{\text{mat}} n_{\text{mat}} \alpha_{\text{mat}} |E|^2 dA}{\left| \int_{\text{all}} \frac{1}{2} (E \times H^*) z dA \right|}, \text{ cm}^{-1}, \quad (5)$$

where  $n_{\text{mat}} = 1.53$  and  $\alpha_{\text{mat}} = 0.2 \text{ cm}^{-1}$  are the REIX and bulk absorption parameter of zeonex.  $\mu_0$  and  $\epsilon_0$  are the free space permeability and permittivity.

The numerical aperture (NA) is the largest allowable angle of incidence of injected light. The NA value depends on EA, light speed ( $c$ ), and operation frequency ( $f$ ). Since it measures how well a fiber can confine radiation, a greater value for it is anticipated. NA is given by<sup>17</sup>

$$NA = (1 + \pi f^2 A_{\text{eff}} / c^2)^{-1/2}. \quad (6)$$

### IV. RESULTS

In this section, the performance of the PCF sensor is examined numerically. Four chemical materials are considered, namely,  $\text{SiCl}_4$ ,  $\text{CCl}_4$ ,  $\text{C}_{10}\text{H}_{16}$ , and  $\text{SnCl}_4$ . To measure the effectiveness of the designed PCF sensor, some optical properties (effective mode index, power factor, relative sensitivity, effective area, numerical aperture, effective material loss, and confinement loss) are investigated in the spectral region of 1–2 THz. The main aim of the current work is the detection of four chemicals ( $\text{SiCl}_4$ ,  $\text{CCl}_4$ ,  $\text{C}_{10}\text{H}_{16}$ , and  $\text{SnCl}_4$ ) in both polarization directions (x-polarized and y-polarized). All the above-mentioned PCF properties depend on the effective mode index that is illustrated in

30 June 2023 09:58:53

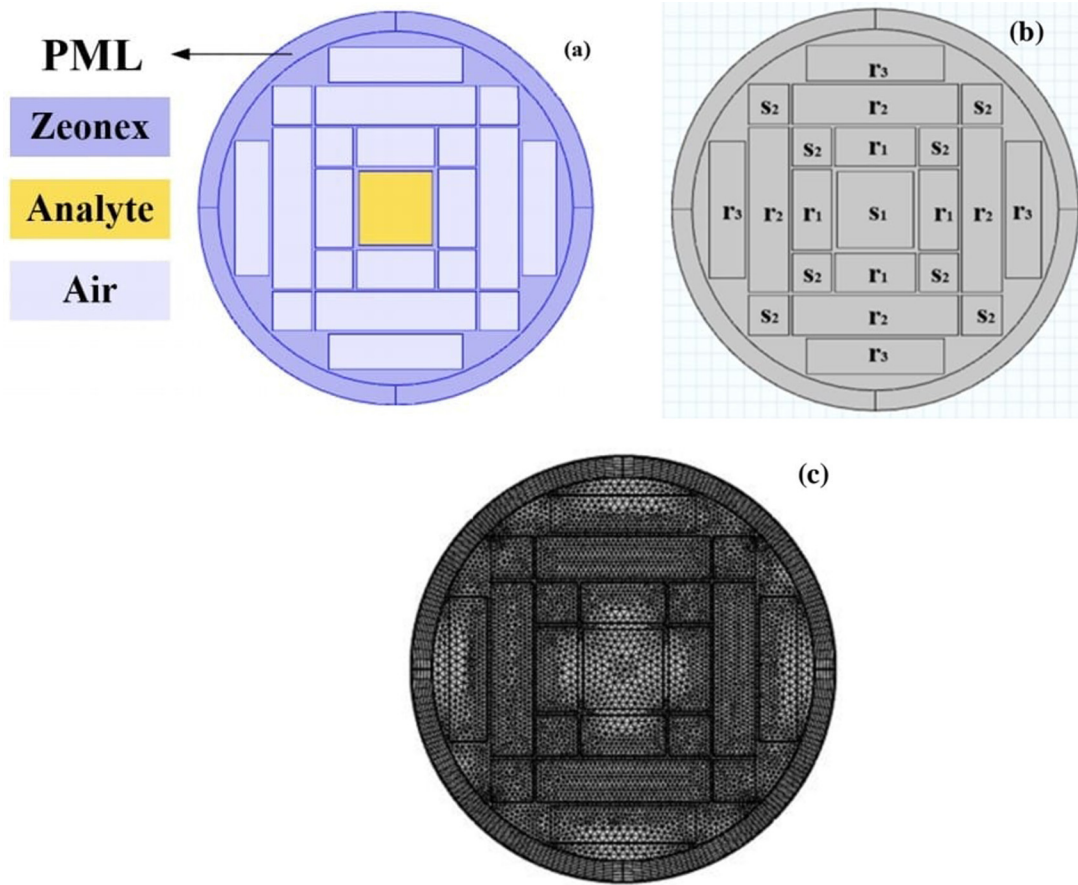


FIG. 1. (a) Cross-sectional representation of the proposed PCF sensor, (b) schematic diagram of the proposed PCF, and (c) extremely fine meshing output with 13 078 domain elements and 1636 boundary elements.

30 June 2023 09:58:53

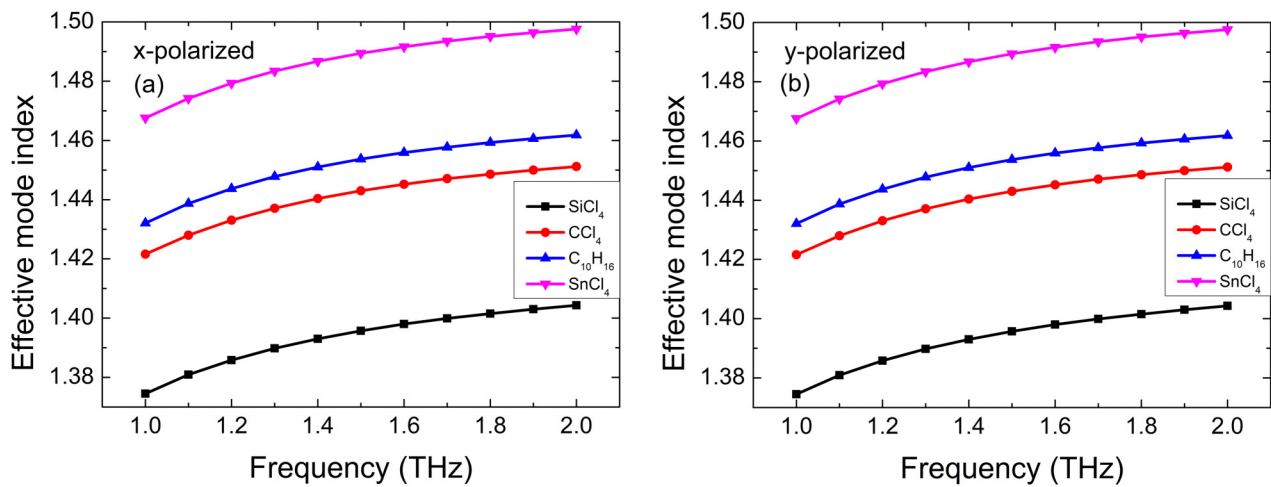
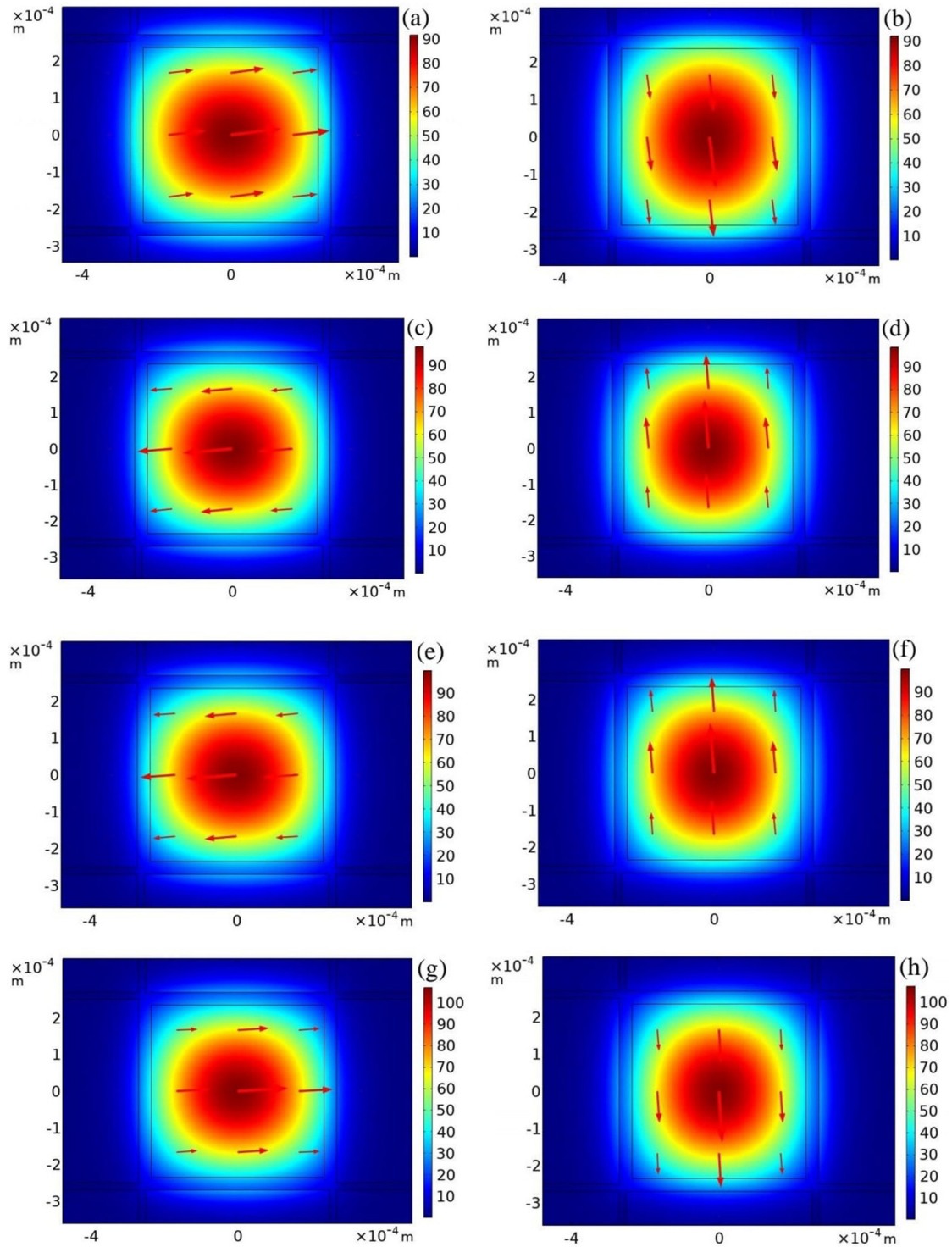


FIG. 2. Effective mode index of SiCl<sub>4</sub>, CCl<sub>4</sub>, C<sub>10</sub>H<sub>16</sub>, and SnCl<sub>4</sub> in (a) x-polarized and (b) y-polarized.



30 June 2023 09:58:53

**FIG. 3.** Representation of the field distribution of the proposed PCF at  $f=1$  THz. x-polarization is shown in Fig. 3 (a), (c), (e), and (g) and y-polarization is shown in Fig. 3 (b), (d), (f), and (h). The analytes are  $\text{SiCl}_4$  (a) and (b),  $\text{CCl}_4$  (c) and (d),  $\text{C}_{10}\text{H}_{16}$  (e) and (f), and  $\text{SnCl}_4$  (g) and (h). The color scales represent the electric field norm (V/m) and the red arrows indicate the magnetic fields.

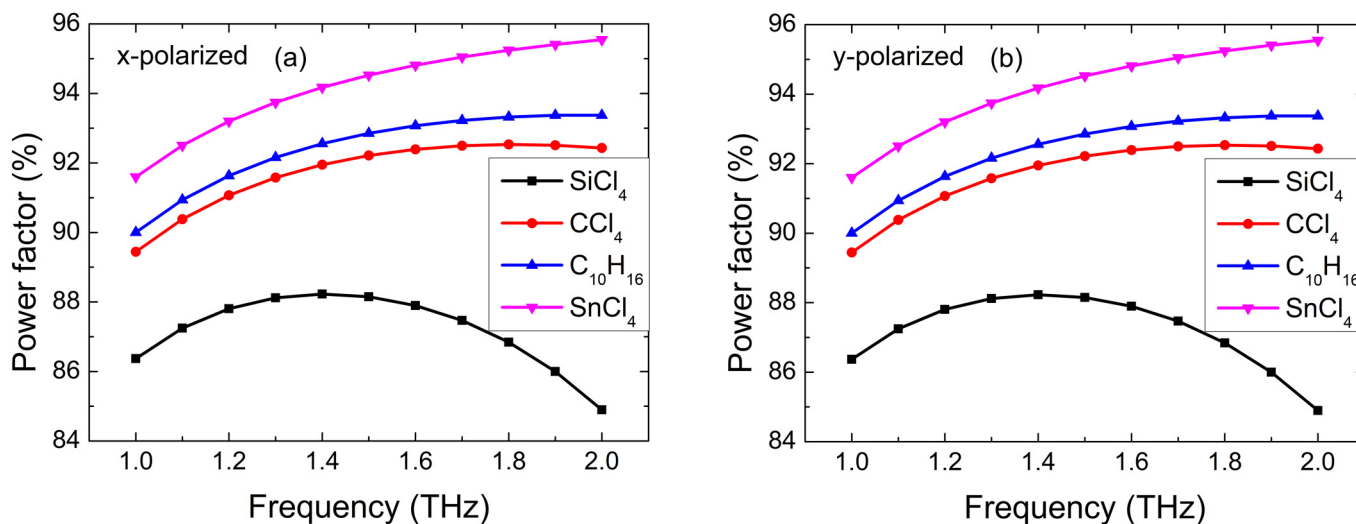


FIG. 4. Power factor of  $\text{SiCl}_4$ ,  $\text{CCl}_4$ ,  $\text{C}_{10}\text{H}_{16}$ , and  $\text{SnCl}_4$  in (a) x-polarized and (b) y-polarized.

Fig. 2 for x- and y-polarizations for all analytes. The effective mode index ranges between 1.375 and 1.49 for all analytes and polarizations, which is relatively close to refractive indices of the analytes. This is a good sign that indicates a sensor of high sensitivity. The mode field distribution for these analytes is displayed in Fig. 3 at 1.9 THz frequency. The figure shows light propagation through these analytes in x- and y-polarizations. Only a small portion of the light leaves the core region; therefore, loss is expected to be limited. The greatest light confinement is displayed in the black-red region. As one approaches the core border, the intensity gradually

decreases, and the red arrow indicates the direction in which light travels. The power fraction as a function of the light frequency is plotted in Fig. 4. Since the light is well-contained inside the square core, the power fraction is high. In x-polarized, 86%, 92.509%, 93.37%, and 95.41% power fractions are, respectively, obtained for  $\text{SiCl}_4$ ,  $\text{CCl}_4$ ,  $\text{C}_{10}\text{H}_{16}$ , and  $\text{SnCl}_4$ , respectively, at 1.9 THz frequency. For y-polarized, the power fractions for  $\text{SiCl}_4$ ,  $\text{CCl}_4$ ,  $\text{C}_{10}\text{H}_{16}$ , and  $\text{SnCl}_4$  are 85.999%, 92.52%, 93.38%, and 95.407%, respectively, at 1.9 THz frequency. For an efficient sensor, the power fraction should be as high as possible.

30 June 2023 09:58:53

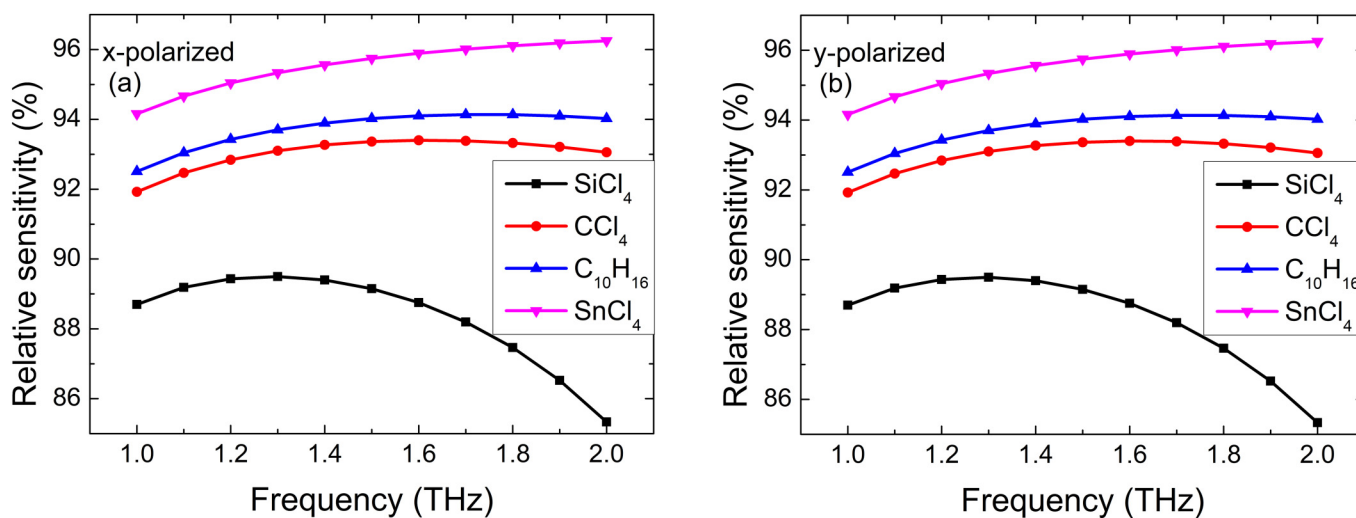


FIG. 5. Relative sensitivity of  $\text{SiCl}_4$ ,  $\text{CCl}_4$ ,  $\text{C}_{10}\text{H}_{16}$ , and  $\text{SnCl}_4$  in (a) x-polarized and (b) y-polarized.

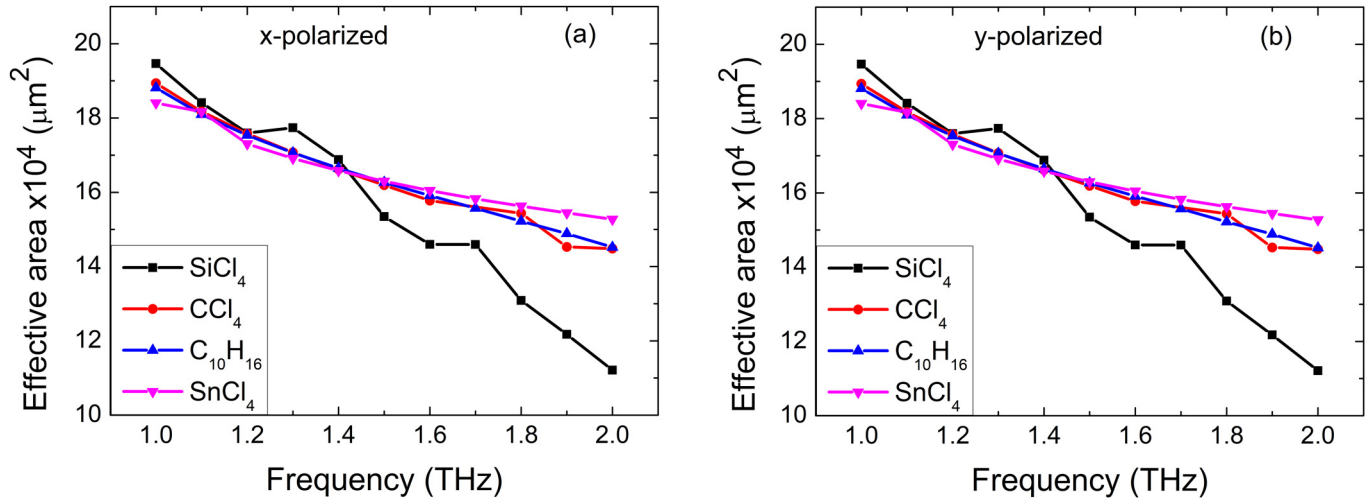


FIG. 6. Effective area of SiCl<sub>4</sub>, CCl<sub>4</sub>, C<sub>10</sub>H<sub>16</sub>, and SnCl<sub>4</sub> in (a) x-polarized and (b) y-polarized.

The main performance parameter is sensitivity, and high sensitivity can be attained by careful design. Figure 5 illustrates the relative sensitivity of SiCl<sub>4</sub>, CCl<sub>4</sub>, C<sub>10</sub>H<sub>16</sub>, and SnCl<sub>4</sub> analytes in x-polarization [Fig. 5(a)] and y-polarized modes [Fig. 5(b)]. In both polarizations, the sensitivity ranges between 86.522% and 96.185% for SiCl<sub>4</sub> and SnCl<sub>4</sub>, respectively. The highest sensitivity of the proposed PCF sensor can be obtained with the SnCl<sub>4</sub> analyte that is extremely high sensitivity. The reason behind the variation in the sensitivity of different analytes is the variation of the REIX. A higher REIX analyte leads to better sensitivity.

The effective area ( $A_{eff}$ ) profile for SiCl<sub>4</sub>, CCl<sub>4</sub>, C<sub>10</sub>H<sub>16</sub>, and SnCl<sub>4</sub> is shown in Fig. 6. The effective area shows a systemic behavior with the frequency. It shows a continuous decrease with increasing frequency. This behavior is due to the compactness of TE mode inside the core zone with increasing frequency. Since the effective area is the region where sensing is most efficient and a high-power density in the zone can be created by lowering the effective area, reduction in  $A_{eff}$  is desired for increasing the sensing performance. Figures 6(a) and 6(b) reveal the effective area of SiCl<sub>4</sub>, CCl<sub>4</sub>, C<sub>10</sub>H<sub>16</sub>, and SnCl<sub>4</sub> for both polarizations, respectively. The effective

30 June 2023 09:58:53

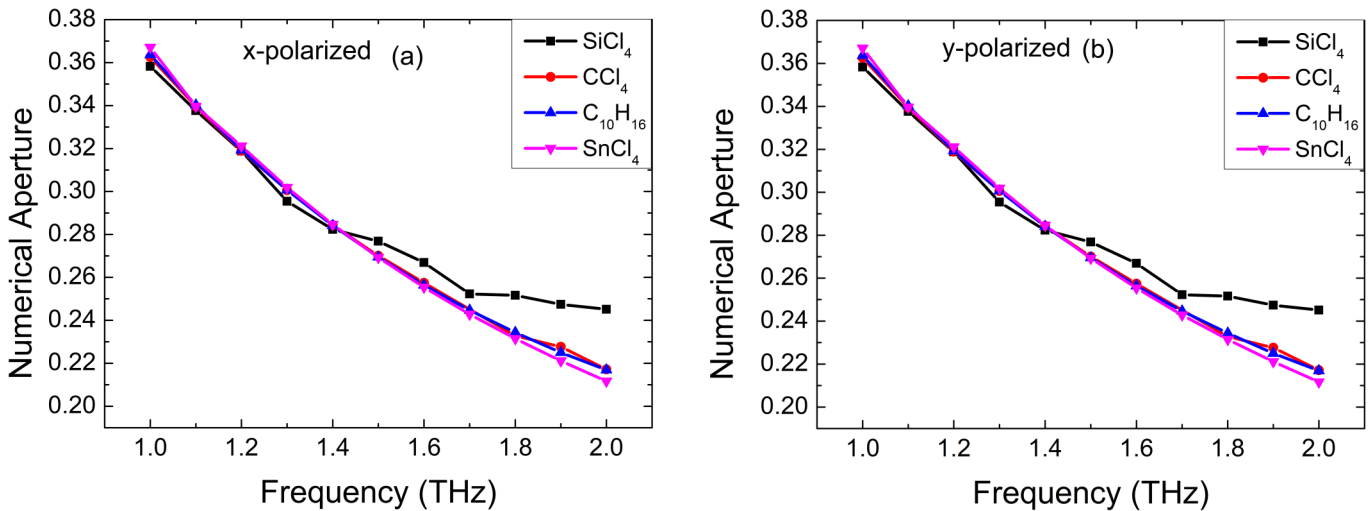


FIG. 7. Numerical aperture of SiCl<sub>4</sub>, CCl<sub>4</sub>, C<sub>10</sub>H<sub>16</sub>, and SnCl<sub>4</sub> in (a) x-polarized and (b) y-polarized.



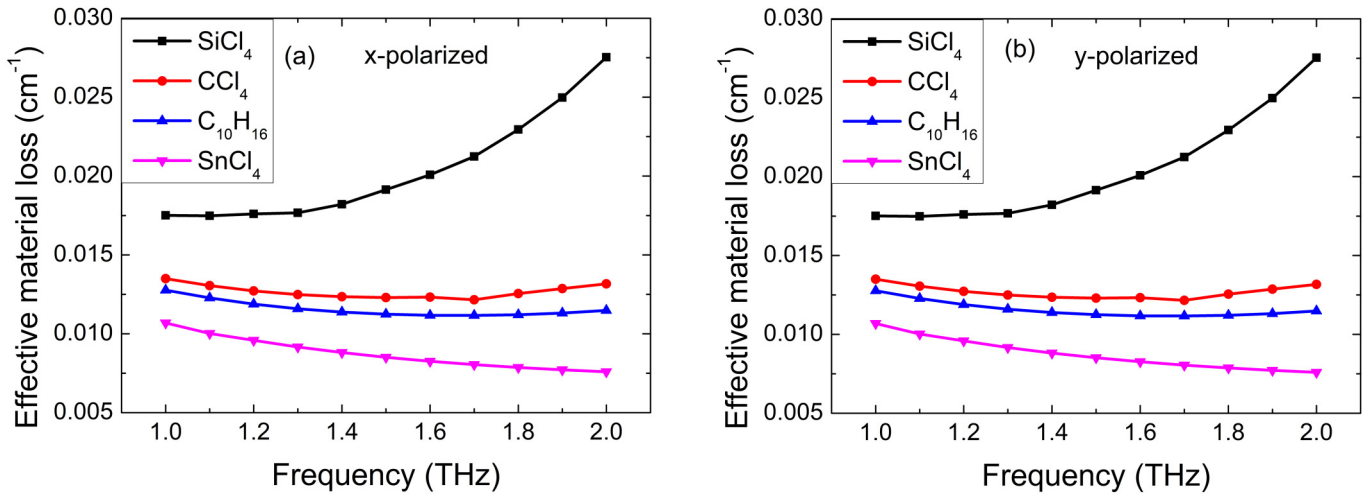


FIG. 8. Effective material loss of  $\text{SiCl}_4$ ,  $\text{CCl}_4$ ,  $\text{C}_{10}\text{H}_{16}$ , and  $\text{SnCl}_4$  in (a) x-polarized and (b) y-polarized.

areas of  $\text{SiCl}_4$ ,  $\text{CCl}_4$ ,  $\text{C}_{10}\text{H}_{16}$ , and  $\text{SnCl}_4$  are 121 760, 145 270, 148 900, and 154 460  $\mu\text{m}^2$  in x-polarized and 121 762, 145 281, 148 903, and 154 471  $\mu\text{m}^2$  in y-polarized, respectively.

The numerical aperture behavior is shown in Fig. 7. It shows a behavior similar to that of the effective area. It also shows a continuous decrease with increasing frequency. It ranges between 0.2 and 0.36 for all analytes for x- and y-polarizations. The best value for the numerical aperture should be as high as possible.

During propagation, each PCF device experiences some losses. Two of the most significant losses are effective material and confinement losses. An efficient PCF sensor must have minimum losses to perform well. The variation in the effective material loss

with the frequency is shown in Fig. 8. Two significant conclusions can be drawn from the figure: (1) the effective material loss exhibits very small values of about 0.0075 to 0.03 and (2) it shows a little dependence on the frequency.

The second type of optical loss that a PCF device experiences through the propagation of light is confinement loss. A very small value of the confinement loss is required. Figure 9 shows the confinement loss of the proposed PCF sensor for the four analytes for x- and y-polarizations. Initially, a higher confinement loss is attained for  $\text{SiCl}_4$  at a frequency of  $f=1$  THz. With the increment in the frequency, the confinement loss decreases and shows neglected values of the order of  $10^{-14}$ . At 1.9 THz frequency, the

30 June 2023 09:58:53

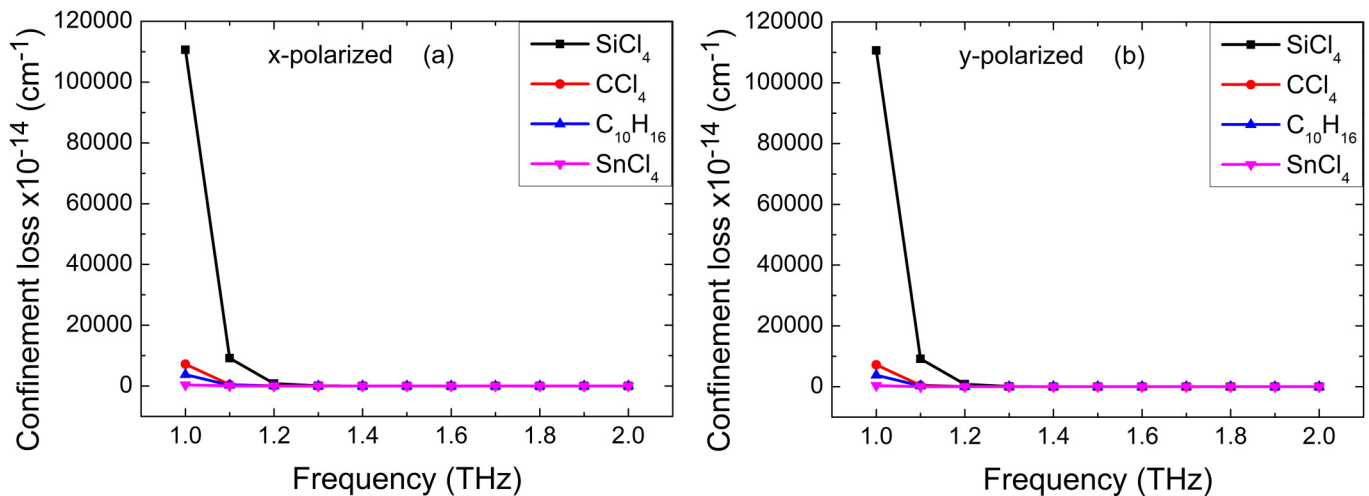


FIG. 9. Confinement loss of  $\text{SiCl}_4$ ,  $\text{CCl}_4$ ,  $\text{C}_{10}\text{H}_{16}$ , and  $\text{SnCl}_4$  in (a) x-polarized and (b) y-polarized.

**TABLE II.** Performance comparison between the most recently published PCFs and the current work.

Reference	RS (%)	$A_{eff}$ ( $\mu\text{m}^2$ )	CL ( $\text{cm}^{-1}$ )	EML ( $\text{cm}^{-1}$ )	PF (%)	NA
24	94.9	...	$1 \times 10^{-6}$	...	...	...
25	56.65	...	$5.32 \times 10^{-4}$	...	...	...
26	95.30	...	...	...	...	...
27	57.61	$10.48 \times 10^5$	...	...	...	...
28	88.65	$5.45 \times 10^5$	$9.162 \times 10^{-10}$	0.005	...	...
29	94.50	...	...	...	...	...
30	81.70	...	$1 \times 10^{-5}$	0.023	...	...
31	91.5	397 340	$4.87 \times 10^{-11}$	0.004	...	...
32	$90 \pm 1$	$5 \times 10^4$	$10^{-16 \pm 1}$	0.02	...	...
33	92.3	209 930	$5.94 \times 10^{-15}$	0.006	...	...
34	92.2	93 754	$6.52 \times 10^{-14}$	0.0117	...	0.194
35	94.2	$3.13 \times 10^5$	$1.28 \times 10^{-13}$	0.0059	93.25	0.177 07
This paper	96.185	154 470	$3.071 \times 10^{-14}$	0.007 72	95.407	0.2211

obtained confinement loss is found as  $2.0994 \times 10^{-14}$ ,  $0.90567 \times 10^{-14}$ ,  $2.2704 \times 10^{-14}$ , and  $4.4567 \times 10^{-14} \text{ cm}^{-1}$  for  $\text{SiCl}_4$ ,  $\text{CCl}_4$ ,  $\text{C}_{10}\text{H}_{16}$ , and  $\text{SnCl}_4$ , respectively, in x-polarized. In y-polarization, the confinement loss is  $0.15581 \times 10^{-14}$ ,  $2.2078 \times 10^{-14}$ ,  $0.48434 \times 10^{-14}$ , and  $3.071 \times 10^{-14} \text{ cm}^{-1}$  for  $\text{SiCl}_4$ ,  $\text{CCl}_4$ ,  $\text{C}_{10}\text{H}_{16}$ , and  $\text{SnCl}_4$ , respectively.

Table II compares several optical characteristics of the current sensor to earlier research in order to show the effectiveness of our suggested sensor. The current PCF sensor shows higher relative sensitivity, higher power fraction, and higher numerical aperture. It also shows a low effective area, effective material loss, and confinement loss compared to most published articles.

## V. CONCLUSIONS

In this work, we have investigated the use of a PCF sensor to identify harmful gases ( $\text{SiCl}_4$ ,  $\text{CCl}_4$ ,  $\text{C}_{10}\text{H}_{16}$ , and  $\text{SnCl}_4$ ). The proposed PCF has a square core and is designed with air cavities in both square and rectangular shapes in the cladding region. The cladding consists of three rings. Four squares and four rectangles are organized in the first ring of the cladding area. Four identical squares and four identical rectangles are grouped in the second ring. The third ring is composed of four rectangles. The fiber has a  $125 \mu\text{m}$  thick PML applied to prevent light scattering from the fiber. The analysis has been conducted using COMSOL 5.6 that is based on the finite element method. The proposed sensor has shown satisfactory performance when operating in the spectral range of 1–2 THz. A relatively high sensitivity of 96.185% along with 95.407% core power fraction, 0.2211 numerical aperture, and a low effective area of  $154\,470 \mu\text{m}^2$  at 1.9 THz frequency have been obtained. Ignorable confinement loss of  $3.071 \times 10^{-14} \text{ cm}^{-1}$  and effective material loss of  $0.007\,72 \text{ cm}^{-1}$  have been also found. When compared with the recently published PCF work, it shows superior performance. After evaluating its performance, we can claim that the proposed sensor can be an effective candidate in the fields of hazardous chemical compound detection, gas detection, and biosensing.

## ACKNOWLEDGMENTS

The authors are thankful to the Deanship of Scientific Research at Najran University for funding this work under the Research Priorities and Najran Research funding program grant code (No. NU/NRP/SERC/12/2).

## AUTHOR DECLARATIONS

### Conflict of Interest

The authors have no conflict to disclose.

### Author Contributions

**Abdulkarem H. M. Almagani:** Software (lead). **Dana N. Alhamss:** Conceptualization (equal); Investigation (equal). **Sofyan A. Taya:** Conceptualization (equal); Supervision (lead); Writing – review & editing (equal). **Ayman Taher Hindi:** Methodology (equal); Writing – review & editing (equal). **Anurag Upadhyay:** Investigation (equal); Methodology (equal). **Shivam Singh:** Investigation (equal); Methodology (equal). **Ihhami Colak:** Formal analysis (equal); Investigation (equal); Methodology (equal). **Amrindra Pal:** Writing – original draft (equal). **Shobhit K. Patel:** Writing – original draft (equal).

## DATA AVAILABILITY

The data that support the findings of this study are available from the corresponding author upon reasonable request.

## REFERENCES

- 1P. Fraser, "Chemistry of stratospheric ozone and ozone depletion," *Aust. Meteorol. Mag.* **46**(3), 185–193 (1997).
- 2A. R. J. Genge, W. Levason, R. Patel *et al.*, "Hydrates of tin tetrachloride," *Acta Crystallogr. Sect. C* **60**(4), i47–i49 (2004).
- 3A. B. Gomez, S. Rubio, and D. P. Bendito, "Analytical methods for the determination of bisphenol A in food," *J. Chromatogr. A* **1216**(3), 449–469 (2009).

- <sup>4</sup>R. H. Jibon, A. A. M. Bulbul, and M. E. Rahaman, "Numerical investigation of the optical properties for multiple PCF structures in the THz regime," *Sens. Bio-Sens. Res.* **32**, 100405 (2021).
- <sup>5</sup>R. H. Jibon, M. Ahmed, M. E. Rahaman, M. K. Hasan, M. M. Shaikh, and A. Tooshil, "Nicotine sensing by photonic crystal fiber in THz regime," in *2nd International Conference on Robotics, Electrical and Signal Processing Techniques* (IEEE ASME Trans. Mechatron, 2021), pp. 337–340.
- <sup>6</sup>A. A. M. Bulbul, R. H. Jibon, S. Biswas, S. T. Pasha, and M. A. Sayeed, "Photonic crystal fiber-based blood components detection in THz regime design and simulation," *Sens. Int.* **2**, 100081 (2021).
- <sup>7</sup>A. A. M. Bulbul, R. H. Jibon, S. K. Das, T. Roy, A. Saha, and M. B. Hossain, "PCF based formalin detection by exploring the optical properties in THz regime," *Nanosci. Nanotech. Asia* **11**(3), 314–321 (2021).
- <sup>8</sup>R. H. Jibon, M. Ahmed, and M. K. Hasan, "Identification of detrimental chemicals of plastic products using PCF in the THz regime," *Meas. Sens.* **17**, 100056 (2021).
- <sup>9</sup>M. S. Hossain, S. Sen, and M. M. Hossain, "Design of a chemical sensing circular photonic crystal fiber with high relative sensitivity and low confinement loss for terahertz (THz) regime," *Optik* **222**, 165359 (2020).
- <sup>10</sup>S. Sen, M. Abdullah-Al-Shafi, A. S. Sikder, M. S. Hossain, and M. M. Azad, "Zeonex based decagonal photonic crystal fiber (D-PH CF) in the terahertz (THz) band for chemical sensing applications," *Sens. Bio-Sens. Res.* **31**, 100393 (2021).
- <sup>11</sup>M. I. Islam, K. Ahmed, M. S. Islam, B. K. Paul, S. Sen, S. Chowdhury, S. Asaduzzaman, A. N. Bahar, and M. B. A. Miah, "Single-mode spiral shape fiber based liquid sensor with ultra-high sensitivity and ultra-low loss: Design and analysis," *Karbala Int. J. Mod. Sci.* **3**(3), 131–142 (2017).
- <sup>12</sup>A. Upadhyay, S. Singh, D. Sharma, and S. A. Taya, "A comprehensive study of large negative dispersion and highly nonlinear perforated core PCF: theoretical insight," *Phys. Scr.* **97**, 065504 (2022).
- <sup>13</sup>S. Sen and K. Ahmed, "Design of terahertz spectroscopy based optical sensor for chemical detection," *SN Appl. Sci.* **1**, 1215 (2019).
- <sup>14</sup>S. Sen, S. Chowdhury, K. Ahmed, and S. Asaduzzaman, "Design of a porous cored hexagonal photonic crystal fiber based optical sensor with high relative sensitivity for lower operating wavelength," *Photonic Sens.* **7**(1), 55–65 (2017).
- <sup>15</sup>S. Chowdhury, S. Sen, K. Ahmed, B. K. Paul, M. B. A. Miah, S. Asaduzzaman, M. S. Islam, and M. I. Islam, "Porous shaped photonic crystal fiber with strong confinement field in sensing applications: Design and analysis," *Sens. Bio-Sens. Res.* **13**, 63–69 (2017).
- <sup>16</sup>B. K. Paul, K. Ahmed, D. Vigneswaran, S. Sen, and M. S. Islam, "Quasi photonic crystal fiber for chemical sensing purpose in the terahertz regime design and analysis," *Opt. Quant. Electron.* **51**(7), 1–12 (2019).
- <sup>17</sup>M. Yin, S. Tang, and M. Tong, "The application of terahertz spectroscopy to liquid petrochemicals detection a review," *Appl. Spectrosc. Rev.* **51**(5), 379–396 (2016).
- <sup>18</sup>M. E. Rahaman, R. H. Jibon, H. S. Mondal, M. B. Hossain, A. A. M. Bulbul, and R. Saha, "Design and optimization of a PCF-based chemical sensor in THz regime," *Sens. Bio-Sens. Res.* **32**, 100422 (2021).
- <sup>19</sup>S. Mohamed Nizar, E. Caroline, and P. Krishnan, "Design and investigation of a high-sensitivity PCF sensor for the detection of sulfur dioxide," *Plasmonics* **16**, 2155–2165 (2021).
- <sup>20</sup>J. N. Dash and R. Jha, "Highly sensitive side-polished birefringent PCF-based SPR sensor in near IR," *Plasmonics* **11**, 1505–1509 (2016).
- <sup>21</sup>H. Liang, Y. Feng, H. Liu *et al.*, "High-performance PCF-SPR sensor coated with Ag and graphene for humidity sensing," *Plasmonics* **17**, 1765–1773 (2022).
- <sup>22</sup>M. S. Hossain and S. Sen, "Design and performance improvement of optical chemical sensor based photonic crystal fiber (PCF) in the terahertz (THz) wave propagation," *Silicon* **13**, 3879–3887 (2021).
- <sup>23</sup>V. Kaur and S. Singh, "Extremely sensitive multiple sensing ring PCF sensor for lower indexed chemical detection," *Sens. Bio-Sens. Res.* **15**, 12–16 (2017).
- <sup>24</sup>M. Niger and T. F. Hasin, "Detection of harmful chemical compounds in plastics with highly sensitive photonic crystal fiber with higher nonlinear coefficient," in *International Conference on Signal Processing, Information, Communication and Systems* (IEEE, 2019), pp. 18–22.
- <sup>25</sup>M. I. Islam, K. Ahmed, S. Sen, S. Chowdhury, B. K. Paul, M. S. Islam, M. B. A. Miah, and S. Asaduzzaman, "Design and optimization of photonic crystal fiber based sensor for gas condensate and air pollution monitoring," *Photonic Sens.* **7**(3), 234–245 (2017).
- <sup>26</sup>J. M. Molina, I. J. Díaz, M. F. Fernández, A. R. Carrillo, F. M. Peinado, V. Mustieles, R. Barouki, C. Piccoli, N. Olea, and C. Freire, "Determination of bisphenol A and bisphenol S concentrations and assessment of estrogen- and antiandrogen-like activities in thermal paper receipts from Brazil, France, and Spain," *Environ. Res.* **170**, 406–415 (2019).
- <sup>27</sup>I. Islam, B. K. Paul, K. Ahmed, R. Hasan, S. Chowdhury, S. Islam, S. Sen, A. N. Bahar, and S. Asaduzzaman, "Highly birefringent single mode spiral shape photonic crystal fiber based sensor for gas sensing applications," *Sens. bio-Sens. Res.* **14**, 30–38 (2017).
- <sup>28</sup>A. A. M. Bulbul, R. H. Jibon, M. A. Awal, E. Podder, H. S. Mondal, M. S. Ahmed, M. B. Hossain, M. M. Hassan, and A. Saha, "Toxic chemicals detection using photonic crystal fiber in THz regime," *11th International Conference on Computing, Communication and Networking Technologies* (IEEE ASME Trans.: Mechatron, 2020), pp. 1–5.
- <sup>29</sup>W. L. C. Liao, M. L. Hou, L. W. Chang, C. J. Lee, W. M. Tsai, L. C. Lin, and T. H. Tsai, "Determination and pharmacokinetics of di-(2-ethylhexyl) phthalate in rats by ultraperformance liquid chromatography with tandem mass spectrometry," *Molecules* **18**(9), 11452–11466 (2013).
- <sup>30</sup>M. S. Islam, J. Sultana, A. Dinovitser, K. Ahmed, B. W. H. Ng, and D. Abbott, "Sensing of toxic chemicals using polarized photonic crystal fiber in the terahertz regime," *Opt. Commun.* **426**, 341–347 (2018).
- <sup>31</sup>B. Abdullah Al-Mamun, H. M. D. Bellal, D. Rahul, and H. Mahadi, "Zeonex-based tetra-rectangular core-photonic crystal fiber for NaCl detection," *Nanosci. Nanotechnol.* **10**, 1–9 (2020).
- <sup>32</sup>F. A. Mou, M. M. Rahman, M. R. Islam, and M. I. H. Bhuiyan, "Development of a photonic crystal fiber for THz wave guidance and environmental pollutants detection," *Sens. Biosens. Res.* **29**, 100346 (2020).
- <sup>33</sup>F. Iqbal, S. Biswas, A. A.-M. Bulbul, H. Rahaman, B. M. Hossain, E. M. Rahaman, and A. M. Awal, "Alcohol sensing and classification using PCF-based sensor," *Sens. Biosens. Res.* **30**, 100384 (2020).
- <sup>34</sup>A. Al-Mamun Bulbul, H. Rahaman, S. Biswas, M. B. Hossain, and A.-A. Nahid, "Design and numerical analysis of a PCF-based bio-sensor for breast cancer cell detection in the THz regime," *Sens. Bio-Sens. Res.* **30**, 100388 (2020).
- <sup>35</sup>R. H. Jibon, E. Md. Rahaman, and M. A. Alahe, "Detection of primary chemical analytes in the THz regime with photonic crystal fiber," *Sens. Bio-Sens. Res.* **33**, 100427 (2021).